AIAA JOURNAL
Vol. 46, No. 9, September 2008

Experimental Study for Momentum Transfer in a Dielectric Barrier Discharge Plasma Actuator

Takashi Abe,* Yuji Takizawa,† and Shunichi Sato‡
Institute of Space and Astronautical Science, Kanagawa 229-8510, Japan
and
Nobara Kimura§
Tokai University, Kanagawa 259-1292, Japan

DOI: 10.2514/1.30985

The momentum-transfer performance of a plasma actuator was investigated experimentally for the effects of ambient-gas pressure, ambient-gas species, and electrode configuration. For measurement of the momentum-transfer performance, the force exerted by the actuator, in addition to the induced velocity, was measured; the consistency between both measurement methods was demonstrated. Results showed that the ambient-gas pressure under which a plasma actuator operates has a considerable effect on the momentum-transfer performance. In fact, the performance does not decrease in a linear manner with decreasing ambient-gas pressure; rather, it initially increases and then decreases. The chemical species of the ambient gas also has a considerable effect on the momentum-transfer performance. The momentum transfer in air is greater than that in nitrogen gas at pressures of less than 1 atm, which suggests a considerable contribution of oxygen molecules in the air. The momentum-transfer performance in carbon dioxide gas is slightly greater than that in nitrogen gas for pressures of less than 1 atm, although they are comparable at 1-atm pressure. Furthermore, the electrode configuration was found to strongly affect the momentum-transfer performance of the plasma actuator. In particular, a mesh-type electrode can improve the performance markedly, compared with the performance of a tape electrode with similar thickness, in an ambient-gas pressure of 1 atm. However, the performance difference attributable to the electrode configuration is greatly reduced with a decrease in the ambient-gas pressure; for example, it almost disappears at pressures of less than approximately 50 kPa.

I. Introduction

RECENTLY, plasma actuators based on the dielectric barrier discharge (DBD) have attracted much attention for several aerospace applications. Furthermore, the DBD itself has a wide range of applications outside of aerospace, such as in materials processing, and therefore has been investigated intensively [1]. For instance, the physical basis of the volume DBD (or double DBD) and its application to surface treatment is detailed in [2]. The most important feature of the DBD is that the corona-to-spark transition can be prevented and the corona discharge is attained even at atmospheric-pressure conditions. In contrast to the volume DBD, the single-DBD plasma actuator (or the surface DBD), which was first proposed by Roth et al. [3–5] and functions as a plasma actuator, is composed of two electrodes and a dielectric plate in between them; one of the electrodes is exposed to ambient gas and the other is encapsulated. The ac high voltage applied to the electrodes can generate a discharge between the exposed electrode edge and the dielectric surface adjacent to the edge even at atmospheric pressure. The resulting surface discharge generates momentum transfer to the ambient gas through collisions between energetic ions and neutral molecules in the ambient gas and induces ambient-gas motion along the surface. Since the time of this pioneering work, the research into DBDs can be classified into two categories. The first is represented by studies that aim to extend the applications of the DBD plasma actuator, and the second includes studies that seek to identify physical mechanisms of the DBD plasma actuator and to investigate means to improve its performance. In the first category, there are many studies that investigate the applicability of the DBD plasma actuator to flow control for flat plates [3,6,7], bluff bodies [8,9], airfoils [10–16], jets [17], mixing layers [18], 3-D vehicles [19–21], and so on. In the second category, many parametric studies have been done experimentally to determine the effect of electrode width, electrode gap, dielectric thickness, electrode thickness, and so on [22–36]. Furthermore, several theoretical investigations have been conducted [37–40]. Despite these efforts, the mechanisms that explain the momentum transfer of the single DBD are still not fully known. For example, most studies of DBD plasma actuators have been performed at atmospheric pressure, but the effect of DBD operation at pressures other than 1 atm is not well understood. This is important, because for applications to high-altitude flight, we must know the performance in a reduced-pressure environment. Furthermore, the information on the performance at pressures other than 1 atm may provide insight into the mechanisms of the DBD plasma actuator. These considerations motivated the current study, which was first presented as an AIAA conference paper [41]. It should be noted that a related paper by another group was presented at the same conference [42], and some of the findings described in this paper were presented concurrently by them.

Previous research suggests that the performance of the DBD plasma actuator depends on the type of surrounding gas. For example, Enloe et al. [22] studied the effect of oxygen/nitrogen fraction and showed that a greater fraction of oxygen improves the DBD actuator performance. In addition, if DBD actuators are to be used on flight vehicles that operate on Mars,¶ then understanding the performance of DBD plasma actuators in a CO_2 environment is also important.

Presented as Paper 187 at the 45th AIAA Aerospace Science Meeting and Exhibit, Reno, NV, 8–11 January 2007; received 13 March 2007; revision received 2 May 2008; accepted for publication 2 May 2008.

*Professor, Space Transportation Engineering Division, 3-1-1 Yoshino-dai, Sagamihara; tabe@gd.isas.jaxa.jp. Associate Fellow AIAA.
†Postdoctoral Researcher, Space Transportation Engineering Division.
‡Technical Staff, Space Transportation Engineering Division.
§Undergraduate Student, Department of Aerodynamics and Astronautics.

¶Data available online at http://marsairplane.larc.nasa.gov/platform.html [retrieved 29 June 2008].

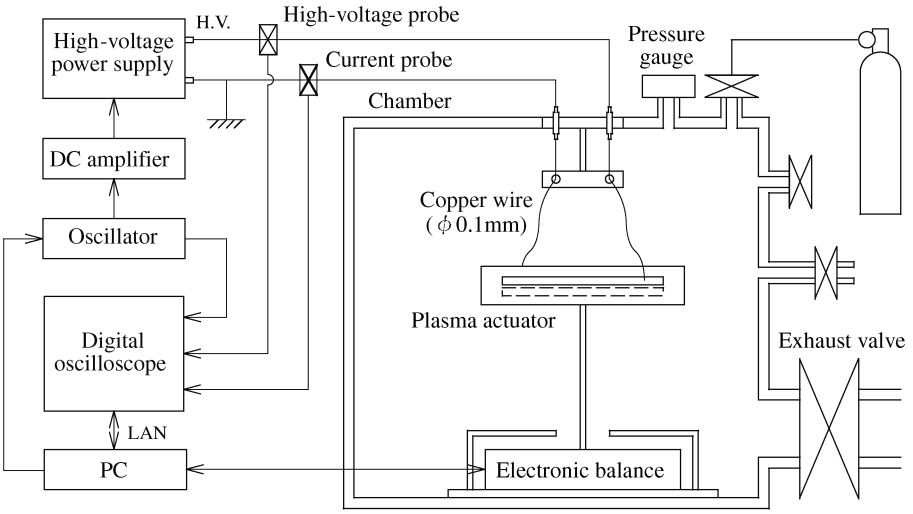

Fig. 1 Experimental setup.

Furthermore, in a previous study [28] at atmospheric-pressure conditions, it was shown that the performance of DBD actuators improved with decreasing thickness of the electrode. This result suggests that there may be room for further improvement of the DBD plasma-actuator performance through modifying the electrode configuration.

With this as motivation, we present here an experimental study in which the performance of the plasma actuator is investigated in a parametric study. In particular, its momentum-transfer characteristics are determined for varying levels of ambient pressure, for various gases, and for various electrode configurations.

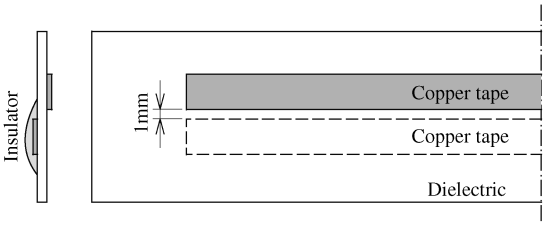

Fig. 2 Schematic for a typical plasma-actuator panel.

II. Experimental Setup

The experimental setup is shown in Fig. 1. The present plasma actuator consists of a pair of electrodes staggered in parallel and a dielectric-plate between them, as shown schematically in Fig. 2. The dielectric plate is made of glass epoxy (glass-fiber-reinforced epoxy) and has a 72-mm chord, 380-mm span, and 1.8-mm thickness. The typical electrodes are identical pieces of metal tape with a 15-mm chord, 300-mm span, and 40-μm thickness. The backside electrode is covered with multilayered Kapton tape to prevent discharge, whereas the front-side electrode is exposed to ambient gas. The gap between the staggered electrodes is 1 mm. On the electrodes, the alternating high voltage, which is generated by amplifying a small signal using an amplifier (10/40A, Trek, Inc.), is applied while the covered electrode is electrically grounded (GND). A ballast register was not used because the discharge in the present study was stable without one. The small signal is generated using a low-voltage general-purpose waveform generator, which enables us to generate an alternating voltage with an arbitrary waveform. Nevertheless, only a sinusoidal waveform was employed for the present study. The effect of different waveforms on the performance of DBD plasma actuators was reported previously using the same experimental setup [41]. The discharge is generated between the exposed electrode and the adjacent dielectric-plate surface, and it induces a flow of ambient gas along the dielectric-plate surface: that is, the momentum transfer to the ambient gas takes place. Generation of the ambient-gas flow causes a response force to the plasma-actuator plate. To quantify the magnitude of the momentum transfer, we measure the response force exerted on the plate using a general-purpose high-precision balance (PB303-s/FACT, Mettler Toledo International. Inc.), with an accuracy of 0.1 mg. The plasma-actuator plate with a stand is directly mounted on the balance. The conducting wires to the electrodes should be as fine as possible to make the response-force measurement as accurate as possible. A wire of 0.1-mm diameter is used for this experiment. The resistance of the wires is less than 0.5 Ω and the power dissipated through them is negligibly small. This was confirmed by varying the length of the wires. That is, only a negligibly small influence on the electric power consumption was observed, even if the length of the wires was doubled.

Along with the response-force measurement, the flow velocity induced by the plasma actuator is also measured. These velocity measurements provide an independent check on the response-force measurements. Note that previous studies have measured the velocity induced by plasma actuators by means of particle image velocimetry or pitot probe [3,24]. Through the measurements, the flow-velocity profile perpendicular to the surface was measured. One problem with particle image velocimetry, however, is that the measurements may be adversely affected by the electrostatic force induced by the high voltage, and pitot tubes, being point measurement devices, are not adequate for quantifying the global momentum change induced by the actuator. Therefore, to measure the global momentum generation of the plasma actuator, the plasma actuator was installed in a channel, as shown in Fig. 3. The channel, which is made of acrylic resin, has a rectangular cross section. Its height and width at the inlet are 5 and 320 mm, respectively. Near the inlet of the channel, the plasma actuator, which is identical to that used for the response-force measurement, is flush-mounted on the lower surface of the channel. The plasma actuator generates the surface flow near the actuator, but near the outlet, the surface flow ultimately develops into an almost-uniform flow over the height of the channel. The channel is made of acrylic resin. Because the height of the induced flow in still air by the plasma actuator is less than 1 mm [24], which is smaller than the height of the channel, the bulk-flow speed after full development over the height becomes too slow to be detected at the outlet if the channel is straight. To overcome this drawback, we employed the converging channel so that the width of the channel outlet is set to be 15 mm. That is, the flow is converged from the 320-mm-wide inlet to the 15-mm-wide outlet, keeping its height of 5 mm. Near the channel outlet, the induced flow velocity is measured by means of a pitot tube. The pitot tube is set at the center of the cross section, and a hole for static pressure is installed through the side wall. The respective outer and inner diameters of the pitot tube are 2 and 1 mm. A differential pressure sensor (KL14, Nagano Keiki Co. Ltd.), of which the accuracy is 50 Pa, is used for measurement of

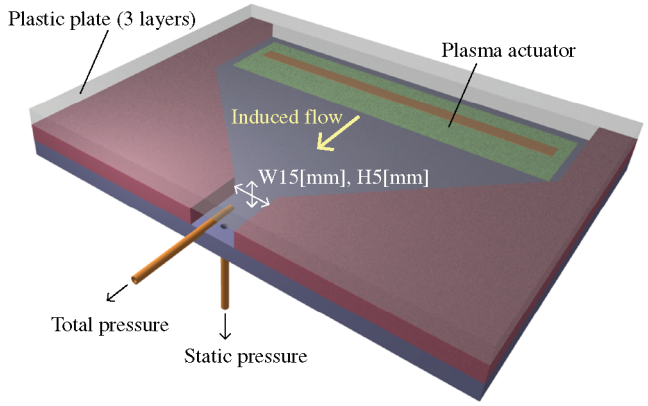

Fig. 3 Setup for velocity measurement of induced flow.

the pressure difference between the pitot tube and the static-pressure hole. The pitot-tube measurement is validated by comparing the measurement of the flow just outside of the outlet by using a conventional flow meter. The accuracy for the velocity determination by the present pitot-tube system is about 0.1 m/s at a 1-atm ambient-pressure condition.

Either the stand with the plasma actuator and the balance or the converging channel with the plasma actuator is set up inside a vacuum chamber that is 1.01 m in diameter and 1.15 m wide. The evacuation chamber enables us to investigate the plasma-actuator performance in a reduced-pressure environment and with different gases. The high voltage applied to the electrode and the electric current through the electrodes are measured using a high-voltage probe (P6015A9, Techtronix) and an electric current probe (701933, Yokogawa Electric Corp.). All data were recorded on a PC and were analyzed after the measurements.

III. Experimental Parameters

In the present experiment, we examine the performance of the momentum transfer for various parameters, as summarized in Table 1. In case 1, the basic performance of the plasma actuator is investigated at an ambient-gas pressure of 1 atm, varying the intensity and frequency of the high voltage. The intensity of the high voltage is defined as its amplitude and varies from 6 to 10 kV. The thrust is below our detectable limit when the amplitude is less than 6 kV with a frequency of 5 kHz. For amplitudes larger than 10 kV, the power consumption may exceed the capability of the high-voltage supply. At the amplitude of 10 kV, the frequency is varied between 1 and 5 kHz. The electrode is made of copper and is 40-μm thick, consistent with previous experiments [28], even though the effect of the thickness will be investigated in case 3. Throughout the present experiment, a sinusoidal waveform is used for the alternating high voltage.

In case 2, the influence of the ambient-gas pressure and species is investigated. As a test gas, we considered air because the DBD plasma actuator is expected to be employed primarily in air and, in fact, most previous investigations dealt with air. Additionally, we consider nitrogen gas because the comparison with the results for air enables us to examine the effect of oxygen in air. Furthermore, we consider CO_2 gas, which is the main component of the Martian atmosphere. Of course, it can be expected that we will see differences in the plasma-actuator performance in a noble-gas atmosphere, but the investigation of this effect will be left to future work.

In case 3, the electrode configuration influence is investigated. As shown in Table 2, the effect of the electrode thickness is investigated in case A, and the effect of a mesh-type electrode is investigated in case B. A stainless steel (SS) mesh (500 mesh/in.) for the mesh electrode is made by weaving wires of 25-μm diameter. As shown in Fig. 4, the mesh electrode has an edge that consists of exposed wires. The pointed wires are expected to enhance the local electric field around the tips and make it stronger than that around the edge of the tape electrode of similar thickness.

Table 2 Electrode materials and configuration

	Electrode	
	Configuration	Thickness
Case A	Copper tape	10 μm
	Copper tape	40 μm
	Copper tape	200 μm
	Copper tape	400 μm
Case B	SUS mesh	25 μm
	SUS tape	30 μm
	Copper tape	40 μm

IV. Results

The typical appearance of the discharge and the temporal behavior of the applied voltage and electric current are depicted, respectively, in Figs. 5 and 6. Here, the ambient-gas pressure is 1 atm, and the amplitude and frequency of the high voltage are 10 kV and 5 kHz, respectively. The discharge region appears over the dielectric surface, starting from the edge of the exposed electrode. The chordwise width of the discharge region in this condition is about 4 mm. The measured electric current is approximately sinusoidal with superimposed high-amplitude random fluctuations that are localized in time. Within one cycle of the alternating voltage, two groups of high-amplitude spikes or pulses are observed. One group appears at the latter half of the up-going voltage phase and the other appears at the latter half of the downgoing voltage phase. The first group exhibits a larger number of pulses than the latter. The superimposed pulses have been observed in previous experiments [27] and have been predicted theoretically as relating to microdischarges [40]. It is widely believed that the plasma associated with the discharge transfers its momentum to the neutral molecules in the surrounding gas. Furthermore, the plasma generated in the negative-going and the positive-going phases of the applied voltage are different in both space and time and cause net momentum transfer downward, as shown in Fig. 5 [24,28]. As a response of the momentum transfer, the present plasma actuator creates upward thrust (also shown in Fig. 5).

A. Typical Behaviors

The experimental parameters considered in this subsection are described as case 1 in Table 1. That is, the amplitude and the frequency of the high voltage are varied, whereas the ambient-gas pressure is set at 1 atm. In Fig. 7, the measured thrust and the electric power consumption are shown for various amplitudes of the applied high voltage. The electric power consumption is calculated by integrating the product of the applied voltage and the electric current

Table 1 Experimental parameters

	Gas species	Pressure P, kPa	Voltage V, kV	Frequency f, kHz	High-voltage electrode material/thickness
Case 1	air	100	6–10	5	Copper/40 μm
	air	100	10	1–5	Copper/40 μm
Case 2	air	25–100	10	5	Copper/40 μm
	N_2	25–100	10	5	Copper/40 μm
	CO_2	25–100	10	5	Copper/40 μm
Case 3	air	25–100	10	2	See Table 2

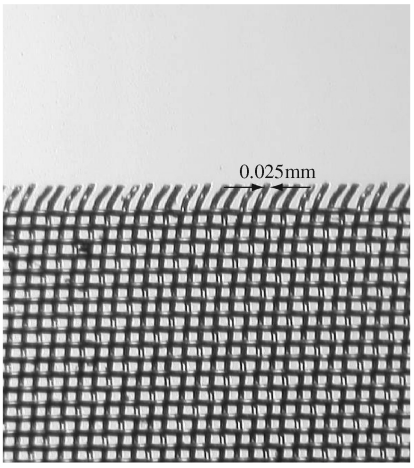

Fig. 4 Microscopic image of the SS mesh electrode and its edge.

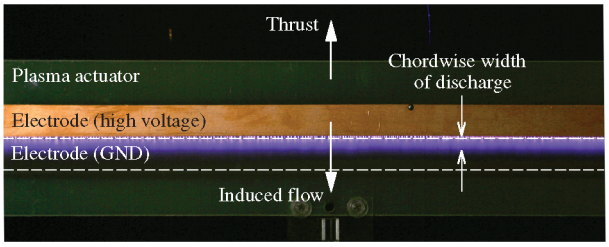

Fig. 5 Typical behavior of the discharge region.

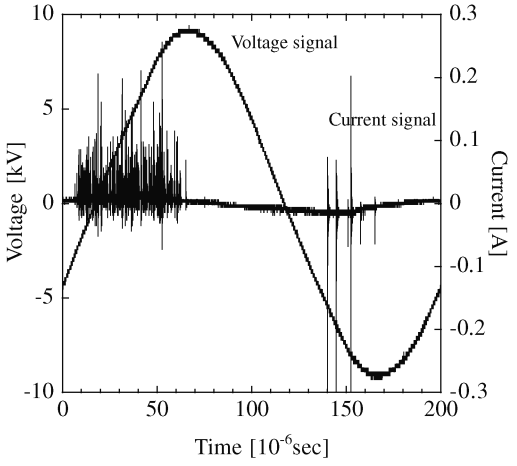

Fig. 6 Typical behavior for a high voltage and electric current.

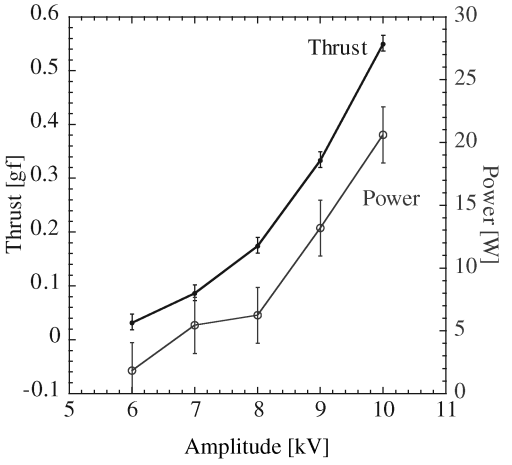

Fig. 7 Generated thrust and consumed power for various amplitudes of the applied high voltage with a frequency of 5 kHz.

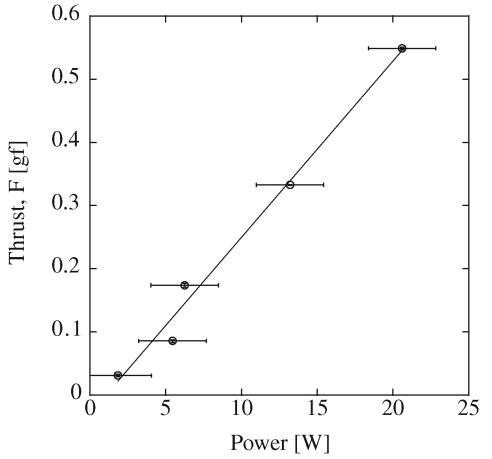

Fig. 8 Relation between the generated thrust and consumed power.

over a period of the alternating high voltage and dividing this integrated quantity by the time period. The figure shows the average power consumption, for which the average was computed from three randomly selected periods of the current-voltage traces. The error bars are defined as the minimum and the maximum values among the three, and the large error bars indicate that there are rather large fluctuations among the power consumptions in each period. Similarly, the measurement of thrust was conducted 3 times and the average thrust is reported in the figure. The error bars represent the minimum and maximum of the measured values of thrust. Both the thrust and the electric power consumption increase with the amplitude of the voltage more rapidly than in a linear manner. Nevertheless, the relation between the thrust and the electric power consumption appears to be linear, as shown in Fig. 8; that is, the thrust increases with the electric power consumption linearly, as previously reported [28]. This means that the part of the electric consumption that is responsible for the response-force generation increases with the total electric consumption.

As the electric power consumption increases, the discharge region becomes brighter, which suggests that a part of the increased electric power contributes to increasing the number of excited molecules and thereby enhancing radiation from them. The pulses in the electric current, which are caused by the presence of microdischarges, become denser and spikier with increasing amplitude of the high voltage. In addition, the noise associated with the discharge increases.

When the frequency of the applied voltage increases, not only the thrust of the plasma actuator, but also the electric power consumption, increases in a roughly linear manner, as shown in Fig. 9, which implies that the momentum transfer and the electric

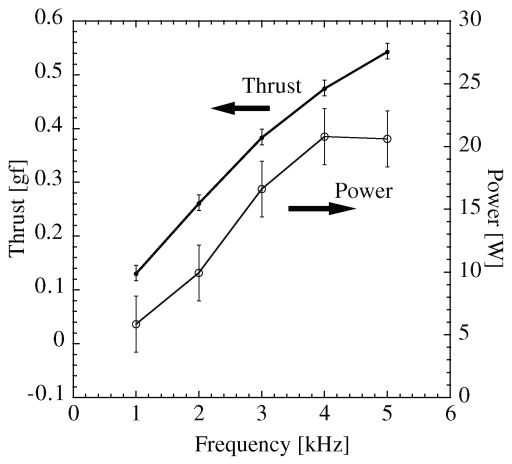

Fig. 9 Generated thrust and consumed power for various frequencies of applied high voltage with amplitude of 10 kV.

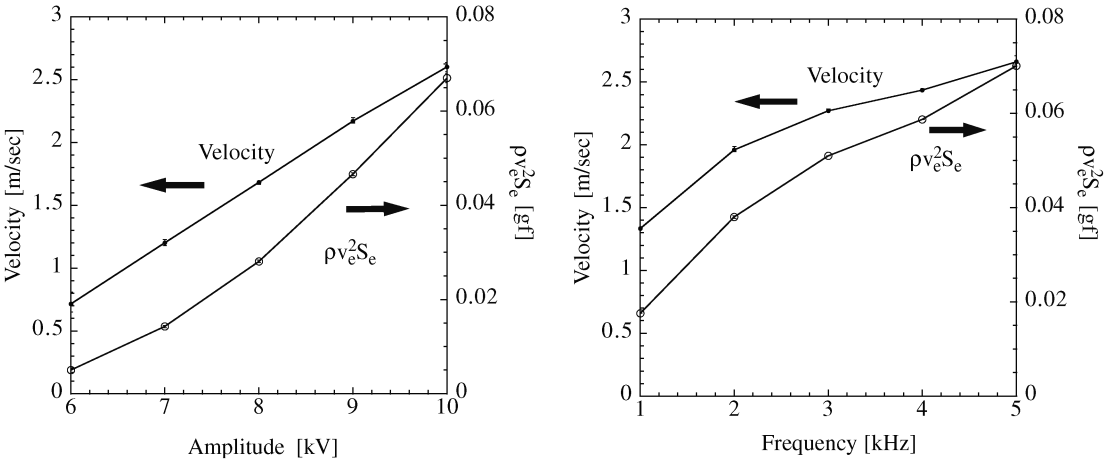

Fig. 10 Induced flow velocity for various amplitudes and frequencies of the applied high voltage.

power consumption in each cycle of the high voltage remain almost the same in this frequency range, as previously shown by Porter et al. [36]. Because of the large error bars for the measurements, the electric consumption at 5 and 4 kHz seems to be equivalent, but it is expected that the electric consumption, like the thrust, actually continues to increase with increasing frequency.

The thrust measured in the present experiment is expected to be generated as a response to the induced flow caused by the plasma actuator. The direct measurement of the induced flow enables us to confirm this expectation. For this purpose, we use a converging channel with a plasma actuator installed near its inlet. The plasma actuator induces a flow only near the surface of the actuator [3,24], but downstream momentum exchange causes the induced velocity to be felt across the height of the channel. In fact, at the exit of the channel, the flow-velocity distribution over the cross section of the outlet becomes almost uniform, except in the boundary layer near the wall. Even though the flow induced by the plasma actuator exhibits a rather low velocity, the effect of the converging channel creates a more readily measurable velocity change, owing to the acceleration of the flow toward the outlet. The measured flow speed v_e at the center of the outlet region is shown in Fig. 10. We can observe a good correlation with the thrust measurement, because the flow velocity becomes larger as both the amplitude and frequency of the applied high voltage increase. It should be noted that because the typical measured flow velocity at the outlet of the converging channel is as low as about 1–2 m/s, the flow induced inside the converging channel is considered to be a fully laminar flow.

The flow momentum caused by the momentum transfer at the plasma actuator should be responsible for the flow momentum at the outlet of the channel, which can be represented by $\rho v_e^2 S_e$. Here, S_e is the cross-sectional area of the outlet. Therefore, we can expect that $\rho v_e^2 S_e$ shows a more direct correlation with the thrust measurement, assuming that the effect of the flow velocity at the inlet of the converging channel and the viscous effect at the converging channel wall are not overwhelming. As shown in Fig. 10, the quantity $\rho v_e^2 S_e$ shows reasonable agreement with the measured thrust, at least qualitatively, even though the quantity $\rho v_e^2 S_e$ is approximately 1 order smaller than the measured thrust because of the momentum dissipation during the flow development along the channel flow. These correlations validate our expectation that the thrust is caused by the flow induced by the plasma actuator.

B. Effect of Ambient Gas

The experimental parameters considered in this subsection are described as case 2 in Table 1. That is, ambient-gas species and pressure are varied, although the amplitude and the frequency of the high voltage are fixed at the values of 10 kV and 5 kHz, respectively. The thrust generated by the plasma actuator is influenced not only by the chemical species in the ambient gas, but also by the pressure of the ambient gas, as shown in Fig. 11. In fact, compared with the thrust

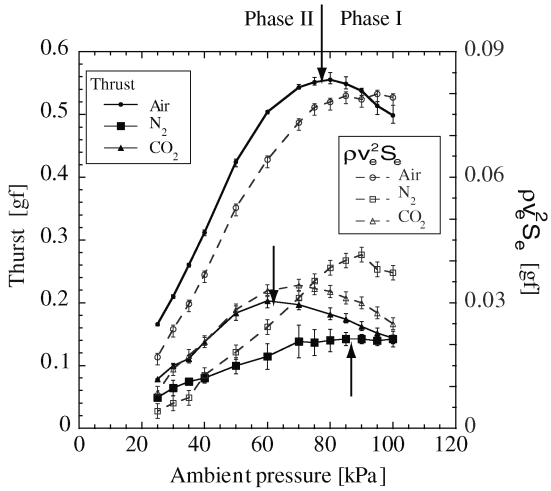

Fig. 11 Thrust level for various ambient-pressure environments and various gases.

level of 0.14 gf for the pure nitrogen gas, the thrust for air is as large as 0.51 gf at 1-atm pressure. The difference in the thrust level between the pure nitrogen gas and air agrees with the previously reported result [22] in which the influence of molecular oxygen in air was intensively investigated. In fact, Enloe et al. [22] showed that the efficiency for air, which is defined as the ratio of the thrust to the electric power consumption, is enhanced compared with that for nitrogen gas and, eventually, the thrust for air is enhanced compared with that for nitrogen gas. They concluded that this difference is attributable to negative ions via attachment of electrons to the oxygen.

For CO_2 gas, the thrust at 1-atm pressure is around 0.14 gf, which is smaller than that for air but comparable with that for pure nitrogen gas. For the volumetric DBD, there are several investigations reporting that CO_2 decomposes into CO and O_2 [43]. But for the DBD plasma actuator, especially for the DBD plasma-actuator performance, the present result is the first one. Nevertheless, the detailed investigations such as that on the components of the generated plasma and its contribution for generating the thrust remain to be done in the future.

When the pressure of the ambient gas was reduced from 1 atm, while maintaining constant amplitude and frequency of the applied voltage, we anticipated that the thrust level would be degraded more or less linearly with the pressure reduction, based on the assumption that the mechanism for the momentum transfer would remain the same. Contrary to that anticipation, the thrust generated by the plasma actuator does not decrease monotonically with pressure reduction, but rather increases initially and then decreases, as shown

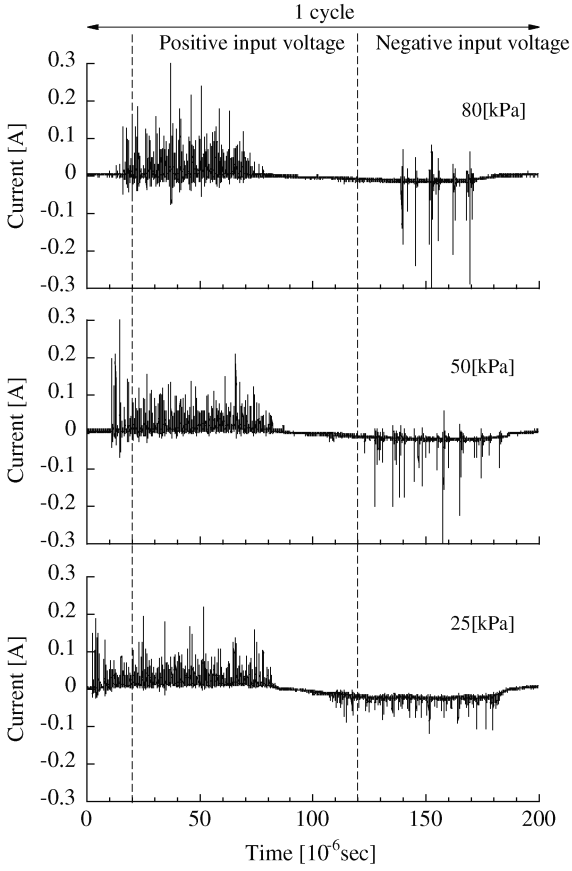

Fig. 12 Typical electric current for various pressure environments.

in Fig. 11. This nonmonotonic behavior differs from expectations and appears to a greater or lesser degree in every gas. This unexpected behavior suggests that the mechanism for the momentum transfer depends, in a complicated manner, on the pressure of the ambient gas. A similar measurement was reported by Gregory et al. [42], who measured the thrust generated by the DBD plasma actuator in a vacuum chamber. In their experiment, the pressure in the chamber was varied between 19 and 78 kPa, but they did not go as high as 101 kPa (or 1 atm) as in the current study. Over their pressure range, they observed a monotonic relationship between the generated thrust and the chamber pressure under the condition of constant electric power consumption. Over the same pressure range, Fig. 11 also shows monotonic variation with the chamber pressure under the condition of constant applied voltage. The nonmonotonic behavior appears in the pressure range of 80–101 kPa, which is just out of the range tested by Gregory et al. [42]. Because we can observe a monotonic relationship between the ambient-gas pressure and the electric power consumption (shown later), we can expect a monotonic relationship between the generated thrust and the electric power consumption, even in our experiment. In this context, both the results agree at least qualitatively.

In addition to the thrust behavior, the effect of the reduced pressure can appear in several other ways. First, the electric current behavior is also affected, as shown in Fig. 12. Lower gas pressure engenders a shorter pulse height and a wider region covered by the pulses. Second, the behavior of the radiating region generated by the discharge is affected. In fact, the radiating region expands when the pressure is reduced, as shown in Fig. 13; that figure presents visible emission images for ambient gases of air, nitrogen, and CO_2, respectively, from left to right. In each column, the plasma-actuator plate without discharge and those with discharge at 100 kPa down to 30 kPa are displayed from top to bottom. For images of the plasma-actuator plate with discharge, the part of the plasma-actuator plate without a discharge is displayed at the right-hand side for comparison. Under 1-atm pressure, the length of the radiating region starting from the edge of the exposed electrode is about 4 mm for both air and CO_2 gas and is around 10 mm for nitrogen gas. The length of the radiating region increases more or less for every gas species when the gas pressure is reduced from 1 atm. Nevertheless, it is noteworthy that it does not extend beyond the edge of the covered electrode. In addition to the increase of the discharge length, we also observe that the plasma region expands normal to the surface and the overall plasma region becomes more diffuse. Third, the electric power consumption in every gas increases, more or less monotonically, with decreasing gas pressure, as shown in Fig. 14. The power consumption was determined as an average over those determined for three arbitrarily chosen periods. The large scatter of the data is attributable to this small sample size. Nevertheless, the trend of power consumption with decreasing gas pressure is evident. When

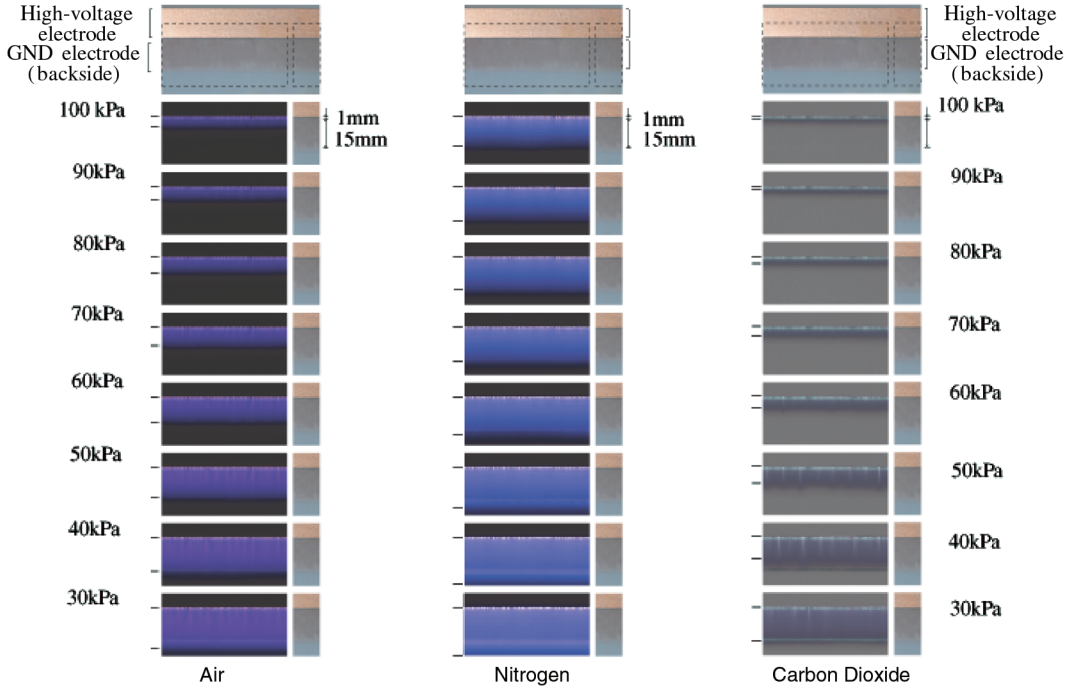

Fig. 13 Influence of ambient-gas pressure on discharge regions.

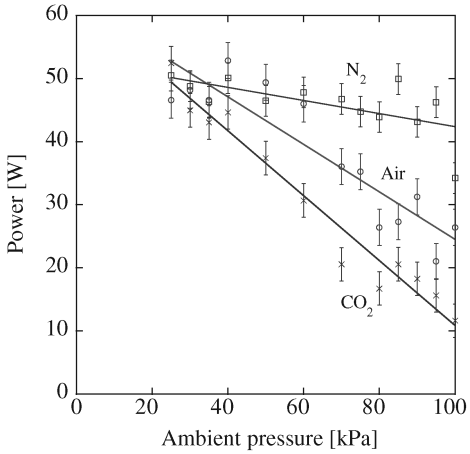

Fig. 14 Power consumption for various ambient-pressure environments and various gases.

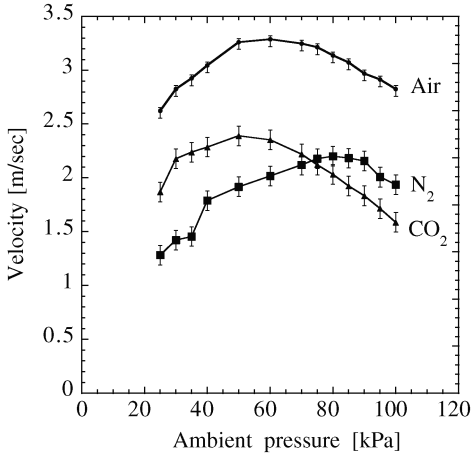

Fig. 15 Induced flow velocity.

the ambient-gas pressure is reduced further, strong sparks appear and the dielectric plate becomes damaged. Sometimes, the strong sparks appear between the wire and the exposed electrode, which leads to wire damage. As a result, the maximum power consumed was limited to about 50 W in every case. The linear trend lines shown in the figure are for reference only and are not intended to imply a known functional relationship. It is noteworthy that the electric power consumption depends on the chemical species of the ambient gas as well. For instance, the power consumption for nitrogen gas is greater than that for air, even though the thrust generation for nitrogen is lower than that for air. The electric power consumption for CO_2 is lower than that for air, which is consistent with the difference in the magnitude of the respective thrust generation.

It is useful to compare the measured thrust with the electric power consumption for varying pressure levels. Previously, we saw that over the range of about 80 to 101 kPa, both the thrust and the electric power consumption increase as the pressure is decreased. We designate this pressure range as phase I. On the other hand, for still lower pressures, the thrust decreases monotonically from its maximum value, whereas the electric power consumption continues to increase. We call this pressure range phase II. In phase I, the discharge behavior is expected to be similar to that observed at 1-atm pressure, because the thrust is nearly proportional to the electric power consumption in both cases.

As discussed previously, this proportionality observed in phase I means that the part of the electric power consumption that is responsible for thrust generation is nearly constant and thus it increases as the pressure is reduced from 1 atm. In contrast, the discharge behavior in the phase-II region differs from that in phase I in that the thrust and the electric power consumption have a negative correlation. That is, the thrust decreases even though the electric power consumption increases. This means that the part of the electric power consumption that is responsible for the thrust generation in phase II is not constant, but smaller. In other words, the more the pressure is reduced, the more electric power is consumed in the processes other than thrust generation. As described previously, the overall plasma region becomes more diffuse when the pressure is reduced. This may suggest that the electric power is dissipated in a larger plasma volume and so the increase of the electric power consumption may not contribute to increasing the thrust generation. From this perspective, the discharge in the phase-II region may become less effective than that in phase I. The preceding hypothesis, however, is only speculative at this time and certainly warrants further investigation.

Regarding the flow-velocity measurement at the exit of the converging channel, the exit flow velocity increases when the pressure is reduced from 1 atm and then decreases, as shown in Fig. 15. That is, the induced flow velocity also shows a nonmonotonic behavior as a function of pressure. As described previously, it is reasonable to investigate the correlation between the measured thrust and the quantity $\rho v_e^2 S_e$. As shown in Fig. 11, the agreement between them is reasonable, at least qualitatively. That is, the nonmonotonic behavior seen in the thrust measurement is also observed in the quantity $\rho v_e^2 S_e$. If the induced velocity were to remain constant in spite of the pressure reduction, then we should observe a monotonic decrease of the quantity $\rho v_e^2 S_e$ against the reduced pressure. Therefore, we can conclude that

1) The nonmonotonic behavior of the measured thrust is caused by the nonmonotonic behavior of the induced flow velocity against the pressure reduction.

2) The decrease of the thrust after the peak value, when the ambient pressure is reduced, is attributable to the decrease in the density of the ambient gas.

C. Effect of Thickness and Configuration of Electrode

Enloe et al. [28] investigated the effect of the thickness of the tape electrode on the plasma-actuator performance in an ambient-pressure environment of 1 atm. They concluded that the induced thrust increased as the electrode was made thinner. In the current work, this study is extended by considering the effect of ambient pressure on the electrode-thickness effect. The experimental parameters considered in this subsection are described as case 3 in Table 1. First, we examine the effect of the tape-electrode thickness and the influence of the ambient-gas pressure, with the amplitude and the frequency of the high voltage fixed at the values of 10 kV and 2 kHz, respectively. As shown in Fig. 16, the current results are in agreement with Enloe et al. for electrodes with thicknesses in the range of 0.01–0.4 mm. That is, at 1-atm ambient-gas pressure, the thinner the electrode thickness, the larger the thrust. However, this effect becomes less clear when the ambient-gas pressure is reduced below 1 atm. In fact, for pressures of less than about 40 kPa, the

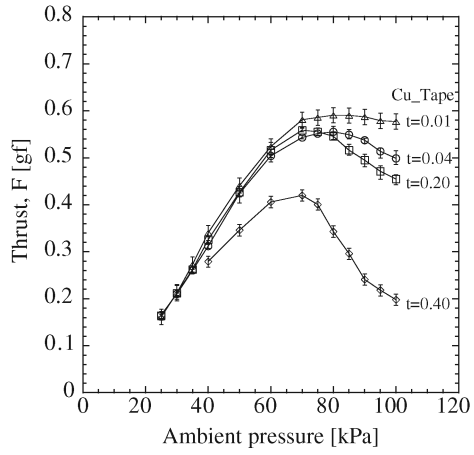

Fig. 16 Generated thrust for various electrode thicknesses.

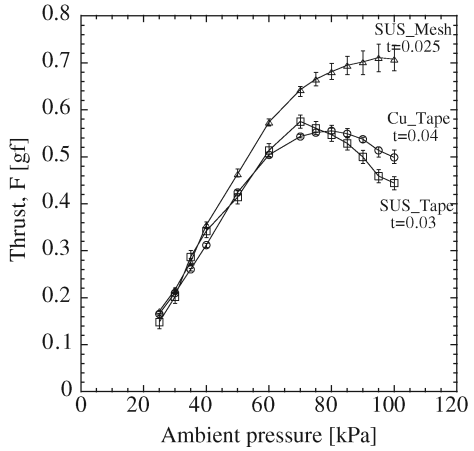

Fig. 17 Generated thrust for various electrode configurations at the high-voltage side.

difference almost disappears; that is, the thrust level in either case becomes comparable and independent of the electrode thickness.

The fact that the thinner electrode improves the performance of the momentum transfer suggests that the stronger local electric field at the edge of the electrode, which is expected for a thinner electrode, might have a strong influence on the improvement of the DBD plasma-actuator performance. Therefore, we can expect that an electrode that can produce a stronger local electric field might improve the performance further. To confirm this expectation, we consider the mesh-type electrodes, which have pointed tips where the wires composing the mesh are exposed, as shown in Fig. 4. We expect enhancement of the local electric field for the pointed wires compared with the sharp two-dimensional edge of the thin tape electrode. In the experiment, the pointed tips of the mesh are 0.025 mm in diameter, which is similar to the tape electrode, for which the thickness is 0.03 mm. As expected, a marked improvement is apparent for the thrust generation, as shown in Fig. 17. Compared with the thrust for the case with the SS tape electrode of 0.03-mm thickness, the thrust for the case with the SS mesh electrode with a similar thickness is more than 50% greater. This enhancement, however, lessens with decreasing ambient-gas pressure. This behavior can be reiterated as follows: the produced thrust increases initially and then decreases, more or less, as described previously when the ambient-gas pressure decreases from 1 atm. However, the appearance of this behavior depends on the electrode configuration. In fact, the local maximum that occurs in the thrust near 80 kPa for the tape electrodes does not occur for the mesh-type electrode.

V. Conclusions

The momentum-transfer performance of a DBD plasma actuator was investigated experimentally for various parameters, including ambient-gas pressure, ambient-gas species, and electrode configuration. The following are the salient results.

1) Both the response-force measurement and the induced velocity measurement are mutually consistent and are verified to be reasonable measurements for the momentum-transfer performance of the plasma actuator.

2) The ambient-gas pressure under which a plasma actuator operates has a considerable effect on the momentum-transfer performance. In fact, the momentum-transfer performance does not decrease monotonically with decreasing gas pressure, but first increases and then decreases. Aside from the momentum-transfer performance, the pressure reduction affects the discharge characteristics such as the appearance of the discharge volume and the electric power consumption behavior. In particular, the electric power consumption was shown to monotonously increase with decreasing ambient-gas pressure. That is, with increasing electric power consumption, the momentum-transfer performance increases at the pressure region near 1 atm, but decreases at lower pressures.

3) The chemical species of the ambient gas has a considerable effect on the momentum-transfer performance. The momentum transfer in air was shown to be greater than that in nitrogen gas for pressures less than 1 atm, which suggests that oxygen strongly influences the characteristics of the actuator. The momentum-transfer performance in carbon dioxide gas was investigated and found to be comparable with that of nitrogen at 1-atm pressure. However, at reduced pressure, the momentum transfer in carbon dioxide was found to be slightly larger than that in nitrogen gas. In general, the differences in the performance characteristics of the different ambient gases tended to diminish with decreasing ambient-gas pressure.

4) The electrode configuration is important for momentum-transfer performance in a plasma actuator. Among tape electrodes, it was shown that thinner tape electrodes were associated with enhanced momentum transfer. Furthermore, results showed that a mesh-type electrode improved the momentum-transfer performance considerably. For example, at a pressure of 1 atm, the momentum transfer for the mesh-type electrode was 150% greater than that of a tape electrode with equivalent thickness. The difference among all of them, however, tended to decrease rapidly with decreasing ambient-gas pressure. In fact, the difference almost disappears at pressures of less than about 50 kPa.

References

[1] Gibalov, V. I., and Pietsch, G. J., "The Development of Dielectric Barrier Discharges in Gas Gaps and on Surfaces," *Journal of Physics D: Applied Physics*, Vol. 33, 2000, p. 2618. doi:10.1088/0022-3727/33/20/315

[2] Wagner, H. E., Brandenburg, R., Kozlov, K. V., Sonnenfeld, A., Michel, P., and Behnke, J. F., "The Barrier Discharge: Basic Properties and Applications to Surface Treatment," *Vacuum*, Vol. 71, No. 3, 2003, pp. 417–436. doi:10.1016/S0042-207X(02)00765-0

[3] Roth, J. R., Sherman, D. M., and Wilkinson, S. P., "Boundary Layer Flow Control with a One Atmosphere Uniform Glow Discharge Surface Plasma," AIAA Paper 98-0328, 1998.

[4] Roth, J. R., "Electrohydrodynamically Induced Airflow in a One Atmosphere Uniform Glow Discharge Surface Plasma," *1998 IEEE International Conference on Plasma Science*, Inst. of Electrical and Electronics Engineers, Piscataway, NJ, 1998.

[5] Roth, J. R., Sherman, D. M., and Wilkinson, S. P., "Electrohydrodynamic Flow Control with a Glow-Discharge Surface Plasma," *AIAA Journal*, Vol. 38, No. 7, 2000, pp. 1166–1172.

[6] Jukes, T. N., Choi, K. S., Jonhson, G. A., and Scott, S. J., "Turbulent Boundary Layer Control for Drag Reduction Using Surface Plasma," AIAA Paper 2004-2216, 2004.

[7] Jukes, T. N., Choi, K. S., Johnson, G. A., and Scott, S. J., "Turbulent Drag Reduction by Surface Plasma Through Spanwise Flow Oscillation," AIAA Paper 2006-3693, 2006.

[8] Thomas, F. O., Kozlov, A., and Corke, T. C., "Plasma Actuators for Bluff Body Flow Control," AIAA Paper 2006-2845, 2006.

[9] McLaughlin, T. E., Munska, M. D., Vaeth, J. P., Dauwalter, T. E., Goode, J. R., and Siegel, S. G., "Plasma-Based Actuators for Cylinder Wake Vortex Control,"AIAA Paper 2004-2129, 2004.

[10] Shcherbakov, Y. V., Isanov, N. S., Baryshev, N. D., Frolovskij, V. S., and Syssoev, V. S., "Drag Reduction by AC Streamer Corona Discharges Along a Wing-Like Profile Plate," AIAA Paper 2000-2670, 2000.

[11] Post, M. L., and Corke, T. C., "Separation Control on High Angle of Attack Airfoil Using Plasma Actuators," AIAA Paper 2003-1024, 2003.

[12] Post, M. L., and Corke, T. C., "Separation Control Using Plasma Actuators-Stationary and Oscillating Airfoils," AIAA Paper 2004-0841, 2004.

[13] Post, M. L., and Corke, T. C., "Separation Control Using Plasma Actuators-Dynamic Stall Control on an Oscillating Airfoil," AIAA Paper 2004-2517, 2004.

[14] Corke, T. C., He, C., and Patel, M. P., "Plasma Flaps and Slats: An Application of Weakly-Ionized Plasma Actuators," AIAA Paper 2004-2127, 2004.

[15] Post, M. L., and Corke, T. C., "Overview of Plasma Flow Control: Concepts, Optimization and Applications," AIAA Paper 2005-0563, 2005.

[16] Corke, T. C., Mertz, B., and Patel, M. P., "Plasma Flow Control Optimized Airfoil," AIAA Paper 2006-1208, 2006.

[17] Samimy, M., Adamovich, I., Webb, B., Kastner, J., Hileman, J., Keshav, S., and Palm, P., "Development and Characterization of Plasma Actuators for High-Speed Jet Control," *Experiments in Fluids*, Vol. 37, No. 4, 2004, pp. 577–588. doi:10.1007/s00348-004-0854-7

[18] Labergue, A., Leger, L., Moreau, E., Touchard, G., and Bonnet, J. P., "Experimental Study of the Detachment and the Reattachment of an Airflow Along an Inclined Wall by a Surface Corona Discharge—Application to a Plane Turbulent Mixing Layer," *IEEE Transactions on Industry Applications*, Vol. 40, No. 5, 2004, pp. 1205–1214. doi:10.1109/TIA.2004.834056

[19] Vorobiev, A. N., Rennie, R. M., Jumper, E. J., and McLaughlin, T. E., "An Experimental Investigation of Lift Enhancement and Roll Control Using Plasma Actuators," AIAA Paper 2006-3383, 2006.

[20] Patel, M. P., Ng, T. T., Vasudevan, S., Corke, T. C., and He, C., "Plasma Actuators for Hingeless Aerodynamic Control of Unmanned Air Vehicle,"AIAA Paper 2006-3495, 2006.

[21] Goeksel, B., and Rechenberg, I., "Active Separation Flow Control Experiments in Weakly-Ionized Gas," *Advances in Turbulence 10*, International Center for Numerical Methods in Engineering, Paper 086H, 2004.

[22] Enloe, C. L., McLaughlin, T. E., Font, G. I., and Baughn, J. W., "Parameterization of Temporal Structure in the Single Dielectric-Barrier Aerodynamic Plasma Actuator," *AIAA Journal*, Vol. 44, No. 6, 2006, pp. 1127–1136. doi:10.2514/1.16297

[23] Forte, M., Leger, L., Pons, J., Moreau, E., and Touchard, G., "Plasma Actuators for Airflow Control: Measurement of the Non-Stationary Induced Flow Velocity," *Journal of Electrostatics*, Vol. 63, Nos. 6–10, 2005, pp. 929–936. doi:10.1016/j.elstat.2005.03.063

[24] Ponce, J., Moreau, E., and Touchard, G., "Asymmetric Surface Barrier Discharge in Air at Atmospheric Pressure: Electric Properties and Induced Airflow Characteristics," *Journal of Physics D: Applied Physics*, Vol. 38, 2005, pp. 3635–3642. doi:10.1088/0022-3727/38/19/012

[25] Seraudie, A., Aubert, E., Naude, N., and Cambronne, J. P., "Effect of Plasma Actuators on a Flat Plate Laminar Boundary Layer in Subsonic Conditions," AIAA Paper 2006-3350, 2006.

[26] Enloe, C. L., McLaughlin, T. E., VanDyken, R. D., and Fischer, J. C.,"Plasma Structure in the Aerodynamic Plasma Actuator," AIAA Paper 2004-0844, 2004.

[27] Enloe, C. L., McLaughlin, T. E., VanDyken, R. D., and Kachner, K. D., "Mechanisms and Responses of a Single Dielectric Barrier Dielectric Barrier Plasma Actuator: Plasma Morphology," *AIAA Journal*, Vol. 42, No. 3, 2004, pp. 589–604. doi:10.2514/1.2305

[28] Enloe, C. L., McLaughlin, T. E., Van Dyken, R. D., Kachner, K. D., Jumper, E. J., Corke, T. C., Post, M., and Haddad, O., "Mechanisms and Responses of a Single Dielectric Barrier Plasma Actuator: Geometric Effects," *AIAA Journal*, Vol. 42, No. 3, 2004, pp. 595–604. doi:10.2514/1.3884

[29] Forte, M., Jolibois, J., Moreau, E., Touchard, G., and Cazalens, M., "Optimization of a Dielectric Barrier Discharge Actuator by Stationary and Instationary Measurements of the Induced Flow Velocity, Application to Airflow Control," AIAA Paper 2006-2863, 2006.

[30] Roth, J. R., and Dai, X., "Optimization of the Aerodynamic Plasma Actuator as an EHD Electrical Device," AIAA Paper 2006-1203, 2006.

[31] Roth, J. R., Dai, X., Rahel, J., and Shermann, M., "The Physics and Phenomenology of Paraelectric One Atmosphere Glow Discharge Plasma Actuators for Aerodynamic Flow Control," AIAA Paper 2005-781, 2005.

[32] Rivir, R., White, A., Carter, C., and Ganguly, B., "AC and Pulsed Plasma Flow Control," AIAA Paper 2004-0847, 2004.

[33] Hong, D., Dong, B., Bauchire, J. M., and Pouvesle, J. M., "Experimental Study of a Dielectric Barrier Discharge Dedicated to Airflow Controls," *Fifth International Symposium on Non Thermal Plasma Technology (ISNTPT 5)* [CD-ROM], Lab. d'Etudes Aérodynamiques, Univ. of Poitiers, Poitiers, France, June 2006.

[34] Baughn, J. W., Porter, C. O., Peterson, B. L., McLaughlin, T. E., Enloe, C. L., Font, G. I., and Baird, C., "Momentum Transfer for an Aerodynamic Plasma Actuator with an Imposed Boundary Layer," AIAA Paper 2006-168, 2006.

[35] Van Dyken, R., McLaughlin, T. M., and Enloe, C. L., " Parametric Investigations of a Single Dielectric Barrier Plasma Actuator," AIAA Paper 2004-0846, 2004.

[36] Porter, C. O., Baughn, J. W., McLaughlin, T. E., Enloe, C. L., and Font, G. I., "Temporal Measurements on an Aerodynamic Plasma Actuator," AIAA Paper 2006-104, 2006.

[37] Shyy, W., Jayaraman, B., and Andersson, A., "Modeling of Glow Discharge-Induced Fluid Dynamics," *Journal of Applied Physics*, Vol. 92, 2002, pp. 6434–6443. doi:10.1063/1.1515103

[38] Singh, K. P., Roy, S., and Gaitonde, D. V., "Modeling of Dielectric Barrier Discharge Plasma Actuator with Atmospheric Air Chemistry," AIAA Paper 2006-3381, 2006.

[39] Boeuf, J. P., and Pitchford, L. C., "Electrohydrodynamic Force and Aerodynamic Flow Acceleration in Surface Dielectric Barrier Discharge," *Journal of Applied Physics*, Vol. 97, 2005, Paper 103307. doi:10.1063/1.1901841

[40] Boeuf, J. P., Kagmich, Y., Callegari, Th., and Pitchford, L. C., "Electrohydrodynamic Force and Acceleration in Surfaces Discharges," AIAA Paper 2006-3574, 2006.

[41] Abe, T., Takizawa, Y., Sato, S., and Kimura, N., "A Parametric Experimental Study for Momentum Transfer in Plasma Actuator," AIAA Paper 2007-187, 2007.

[42] Gregory, J. W., Enloe, C. L., Font, G. I., and McLaughlin, T. E., "Force Production Mechanisms of a Dielectric-Barrier Discharge Plasma Actuator," AIAA Paper 2007-185, 2007.

[43] Li, R., Tang, Q., Yin, S., Yamaguchi, Y., and Sato, T., "Decomposition of Carbon Dioxide by the Dielectric Barrier Discharge (DBD) Plasma Using $Ca_{0.7}Sr_{0.3}TiO_3$ Barrier," *Chemistry Letters*, Vol. 33, No. 4, 2004, p. 412. doi:10.1246/cl.2004.412

N. Clemens
Associate Editor